GROWTH AND HARDENING OF ALKALI HALIDES FOR USE IN INFRARED LASER WINDOWS

Joel J. Martin, et al

Oklahoma State University

Prepared for:

Air Force Cambridge Research Laboratories
Defense Advanced Research Projects Agency

31 July 1975

AFCRL-TR-75-0432

GROWTH AND HARDENING OF ALKALI HALIDES FOR USE IN INFRARED LASER WINDOWS

by

Joel J. Martin, Charles T. Butler

and William A. Sibley

Department of Physics
Oklahoma State University
Stillwater, Oklahoma 74074

Final Report for Period

1 May 1972 - 31 July 1975

Approved for public release; distribution unlimited.

Sponsored by
Defense Advanced Research Projects Agency
ARPA Order No. 2055
Monitored by
AIR FORCE CAMBRIDGE RESEARCH LABORATORIES
AIR FORCE SYSTEMS COMMAND
UNITED STATE AIR FORCE
HANSCOM AFB, MASSACHUSETTS 01731

Unclassified

Security Classification

DOCUMENT CONTROL DATA - R & D

(Security classification of title, body of abstract and indexing annotation must be entered when the overall report is classified)

1. ORIGINATING ACTIVITY (Corporate author)
Oklahoma State University
Department of Physics
Stillwater, Oklahoma 74074

2a. REPORT SECURITY CLASSIFICATION
Unclassified

2b. GROUP
N/A

3. REPORT TITLE

GROWTH AND HARDENING OF ALKALI HALIDES FOR USE IN INFRARED LASER WINDOWS

4. DESCRIPTIVE NOTES (Type of report and inclusive dates)
Scientific Final for Period 1 May 1972 - 31 July 1975

5. AUTHOR(S) (First name, middle initial, last name)
Joel J. Martin, Charles T. Butler
and William A. Sibley

6. REPORT DATE	7a. TOTAL NO. OF PAGES	7b. NO. OF REFS
31 July 1975	~~54~~ 58	48

8a. CONTRACT OR GRANT NO.	9a. ORIGINATOR'S REPORT NUMBER(S)
F19628-72-C-0306	
b. PROJECT, TASK, AND WORK UNIT NO. 2055 N/A N/A	
c. DOD ELEMENT 61101D	9b. OTHER REPORT NO(S) (Any other numbers that may be assigned this report) AFCRL-TR-75-0432
d. DOD SUBELEMENT N/A	

10. DISTRIBUTION STATEMENT

A. Approved for public release; distribution unlimited

11. SUPPLEMENTARY NOTES	12. SPONSORING MILITARY ACTIVITY
This research was supported by the Defense Advanced Research Projects Agency. ARPA Order No. 2055	Air Force Cambridge Research Laboratories, Hanscom AFB, Massachusetts 01731 Contract Monitor: Major N. Klausutis/LQP

13. ABSTRACT

KCl crystals pulled from pretreated melts under an Ti gettered inert atmosphere have been shown to have as low an absorption as crystals grown by the RAP Bridgman method. A simple optical method has been developed to analyze KCl:Eu for Eu content. Radiation damage significantly increases the 10.6 μm absorption of both KCl and NaCl. The absorption increase is caused by the F-aggregate centers. This result probably rules out the use of radiation strengthened KCl for high power laser window applications. The flow stress of KCl:Eu was found to increase linearly with Eu content. The flow stresses of $KBr_x Cl_{1-x}$ crystals have the same temperature dependence as the flow stress of pure KCl.

i.

DD FORM 1 NOV 65 1473

Unclassified

Security Classification

Unclassified

Security Classification

14 KEY WORDS	LINK A		LINK B		LINK C	
	ROLE	WT	ROLE	WT	ROLE	WT
Alkali Halides						
Pure and doped KCl						
KCl: KBr mixed crystals						
Flow Stress						
Crystal Growth						
Crystal Characterization						
Irradiated KCl						
Irradiated Polycrystalline KCl						

Unclassified

Security Classification

Table of Contents

ARPA Order No. 2055

Program Code No. 2D10

Contractor:
Oklahoma State University

Effective Date of Contract:
1 May 1972

Contract No. F19628-72-C-0306

Principal Investigator & Phone No.:
Dr. William A. Sibley
(405) 372-6211, Ext. 7525

AFCRL Project Scientist & Phone No.:
Major Normantas Klausutis
(617) 861-4841

Contract Expiration Date:
31 July 1975

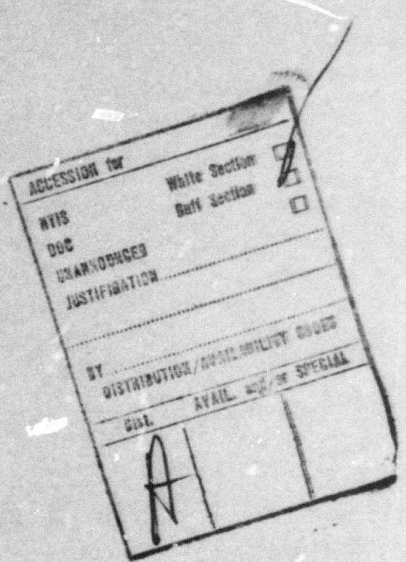

Qualified requestors may obtain additional copies from the Defense Documentation Center. All others should apply to the National Technical Information Service.

I. INTRODUCTION AND SUMMARY

This project was initiated to study the effects of impurity doping and irradiation on the mechanical and optical properties of alkali halides. Our group has concentrated its efforts on KCl, which has been shown to be one of the most promising materials for use in CO_2 laser windows. This report is organized into three general sections which cover the major areas of our efforts. These are:

Crystal Growth: Methods have been developed for growing low absorption KCl ($\beta_{10.6} < 8 \times 10^{-4} cm^{-1}$) both by the RAP-Bridgman technique and by pulling from pretreated melts. For pulled crystals we found that it was necessary to use a Ti-gettered atmosphere in a high vacuum tight system.

The Effect of Ionizing Radiation on the 10.6μm Absorption of KCl and NaCl: We have shown that $\beta_{10.6}$ increases upon irradiation for both KCl and NaCl. For the window project this means that it is impractical to use radiation strengthened alkali halides as window materials. The absorption increase was shown to come from the F aggregate centers rather than from the Cl^o interstitial clusters. This study was done jointly with H. Lipson and P. Ligor of AFCRL.

Mechanical Properties: Both radiation damage and doping by divalent ions were shown to significantly strengthen alkali halides. The temperature dependence of the yield strength of KCl:Sr and KBr_xCl_{1-x} crystals was investigated.

II. CRYSTAL GROWTH

A. Objectives

The crystal-growth phase of this project has three main objectives: 1) to provide single crystals for mechanical and optical measurements of pure, doped, and irradiated KCl. 2) To provide crystals grown by both the Bridgman and pulling techniques from different starting materials in order to determine the effects of these factors. 3) To provide crystals to other laboratories.

B. Crystal Pullers

The two crystal pullers used in this project are described below:

Model I Puller. General features of the Model I Puller are shown in Figure 1. The graphite heater consists of a slotted cylindrical portion and a slotted flat pedestal section, electrically connected in series. In operation, these heaters typically dissipate 250 W at a current of 45 A. The cylindrical heater is maintained at a preset temperature by an external three action controller (Research, Incorporated, Model 625). The sensing element is a type K thermocouple embedded in the cylinder wall. A second thermocouple is used to monitor the pedestal (base) heater temperature. In order to maintain the proper temperature profile in the melt, the base heater is operated 50 to 100^{o}C above that of the cylinder heater. Both heaters are mounted on nickel blocks which are mechanically clamped to the water-cooled base plate by the current feed throughs. BeO washers provide the necessary low electrical and high thermal conductance.

The entire heater assembly is enclosed in a double-walled, water-cooled, stainless steel vacuum jacket. To facilitate observation of the growth interface, a microscope illumination lamp is permanently mounted to one of the three view parts on the top plate. High purity alumina crucibles (Coors Porcelain,

grade AD99) 5cm diameter by 9cm high are presently employed. A water-cooled, stainless steel pullrod with an integral nickel seed chuck is used. A separate seed chuck cannot be used in this system since the heat of solidification is removed through the seed and crystal during a significant portion of the growth process.

The pullrod is rotated at 30 rpm by a small motor located on the lift mechanism. In this way, small radial assymetries in the temperature distribution within the heater volume are smoothed out, and a more symmetric crystal is obtained. The heater and current feedthrough designs are similar to ones in use by F. Rosenberger (1) at the University of Utah. The pullrod, vacuum seals, lift mechanism and other features were developed here.

Pulling is accomplished by moving the pullrod and its rotation motor with a precision lead screw driven by a variable speed motor. Precision linear ball bearings insure smooth motion. The lift rate is directly readable from a calibrated tachometer, and is continuously adjustable from zero up to 1.8cm/hr. An electromechanical clutch allows manual adjustment of the pullrod position when necessary.

Model II Puller. Figure 2 shows the second pulling apparatus. In this design, no thermocouples, heaters or other hardware are mounted within the vacuum enclosure. This results in less contamination of high purity melts and facilitates clean-up after a doped crystal is grown. The only materials which are at full temperature are the crucible, its silica stand, and the high purity silica vacuum enclosure. A type K thermocouple, placed at a suitable level on the outside wall of the silica enclosure, serves as the sensing element for the temperature controller. The same controller is used interchangeably for both pullers. The pullrod and vacuum connections are made to the silica envelope by means of a water-cooled, stainless steel header.

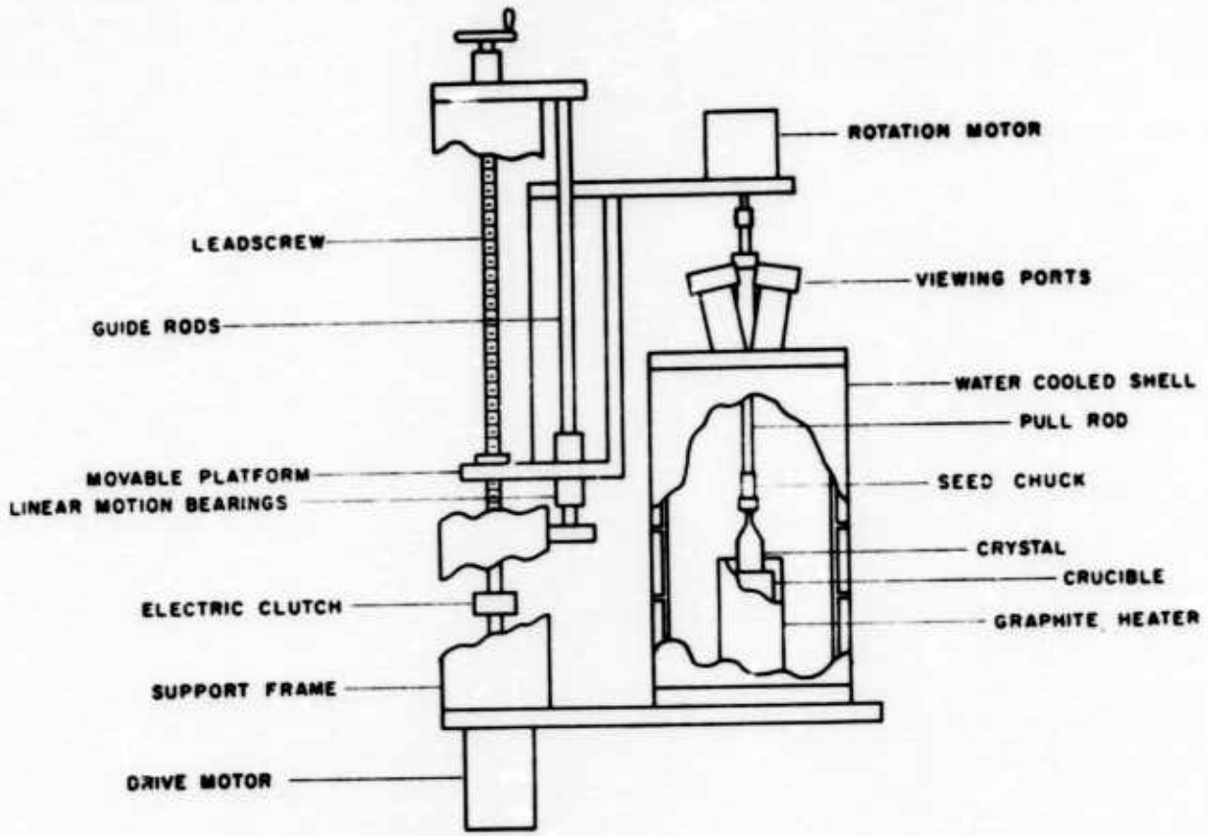

Figure 1. Schematic Diagram of the Model I Puller.

The basic design for this system is similar to one developed by one of the authors (CTB) at Oak Ridge National Laboratory for high purity KCl single crystals (2, 3). The mechanical pulling mechanism and pullrod are essentially identical to those for the first puller.

The vacuum systems for both pullers are separate but identical, sharing only a common fore pump. Each system comprises a 2-inch, water-cooled and baffled diffusion pump (T-M Vacuum Products) and a liquid nitrogen cold trap (Circuits Processing Apparatus). The T-M diffusion pump has a three minute start up and a one minute cool down time. Because operation of these apparatus requires several pump-down and inert gas backfills, this feature results in a considerable time saving.

In a typical growth run using reagent material, approximately 110 g KCl powder is transferred directly from a supply bottle into a crucible. For Sr-doped crystals, the appropriate amount of anhydrous $SrCl_2$ is added. The crucible is then placed in the heater assembly on 20mm ceramic standoffs and carefully centered. A seed 5x5x30mm is secured in the chuck, the apparatus assembled, and the enclosure evacuated to a pressure near 10^{-5} torr. The system is then backfilled once with argon gas, repumped, and baked under hard vacuum overnight at 300°C.

The next morning, the system is flushed with argon gas, repumped to hard vacuum, and the temperature raised to 700°C. Often, one or more additional argon backfills are employed during the hour required to reach this temperature. At 700°C, the system is sealed at a static argon pressure of 20-25 torr absolute. This pressure is sufficient to suppress evaporation from the melt, but insufficient to allow significant convective transport. Thus, the viewports remain clear throughout the growth run. Pulling rates up to 1cm/hr are possible during the early stages of growth in this apparatus, but as the

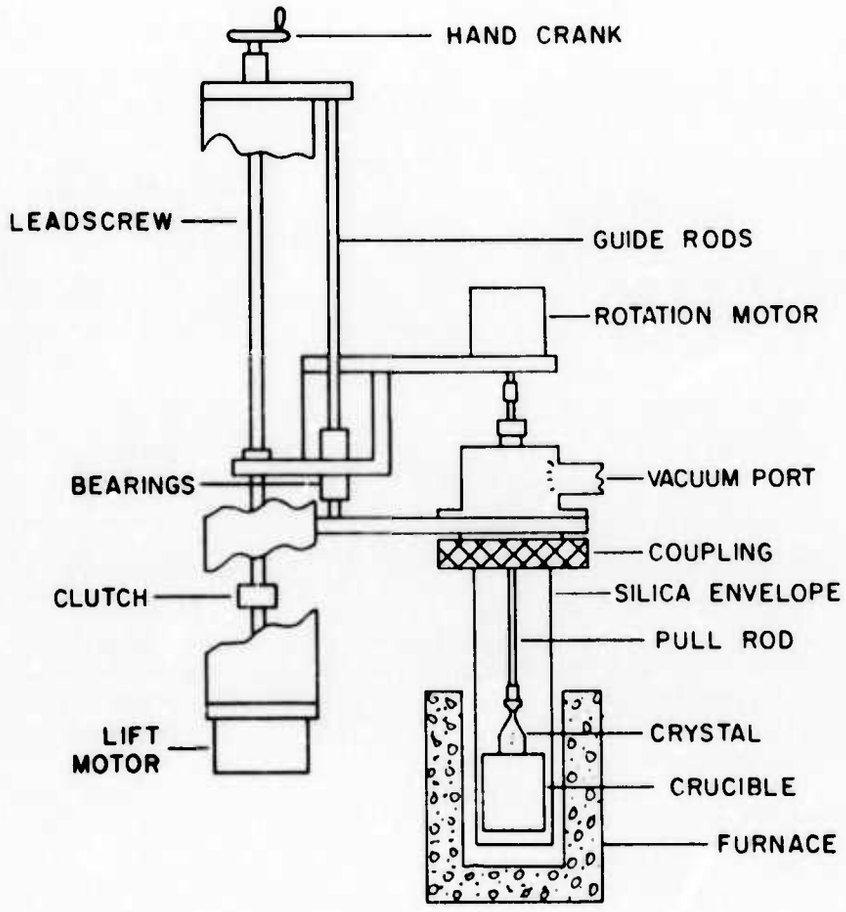

Figure 2. Schematic Diagram of the Model II Puller.

crystal lengthens, pull rates must be lowered because of the lessened heat conductance. Later, as radiative losses from the interface and crystal body become important, pull rates of 1.5cm/hr or greater may be used. A significant difference in the designs of the two pulling apparatus lies in the manner in which the heat of solidification is removed from the growth interface. In the number two puller, radiative losses predominate during the entire growth process, and relatively high pull rates are continuously maintainable.

In previous work, it has been found necessary to use apparatus capable of being evacuated to 10^{-5} torr or below if oxygen compounds are to be excluded from pure crystals, and if unwanted precipitation of dopants is to be avoided in doped runs. That is, if air is allowed to contact the melt during growth, or if the starting material is insufficiently outgassed, pure crystals tend to be oxygen and hydroxyl doped, while doped crystals tend to be purer than desired.

C. Reactive Atmosphere Processing

Since KCl crystals pulled from reagent grade starting material in either of the systems described above had high 10.6μm absorption coefficient ($\geq 3 \times 10^{-3}$ cm^{-1}) we have set up two separate reactive atmosphere processing systems. One of these is a pretreatment system for purifying starting material. The other is a Bridgman crystal growth system that can be used either to grow crystals directly or to pretreat the material for later use in the crystal pullers.

RAP-Pretreatment System

Pastor and Pastor (4) have developed a technique in which CCl_4 vapor in an Ar carrier gas passes past the melt in a Bridgman crystal-growth system. This method, called Reactive-Atmosphere Processing (RAP) yields crystals having 10.6μm absorption coefficients in the low 10^{-4} cm^{-1} range.(4,5) Their method

also has the advantage of simplicity over the more complex HCl/Cl_2 treatment methods reviewed in detail by Rosenberger.(6) Because crystal pullers generally are incompatible with the reactive atmosphere, a modification for pretreatment of reagent grade material has been introduced. Carbon tetrachloride vapor is bubbled through a charge of molten KCl in a separate silica system. Since the bubbling thoroughly mixes the CCl_4 vapor and the molten KCl, the scrubbing reactions should be more complete. When the treatment is completed, the solidified KCl ingot is transferred to the crystal growth system.

This modified RAP treatment is carried out in the system shown in Figure 3. First, a fused silica crucible containing the untreated reagent grade KCl is placed inside a silica chamber. The furnace surrounds the silica chamber so that the KCl is exposed only to silica and CCl_4 vapors in a helium carrier. Dry helium gas passes through the system at about 15 cm^3/min as the KCl is heated and cooled. The furnace temperature is increased 300 C^o/h until the KCl melts and is then held steady at 850 $\pm$ 25^{o}C during the RAP run. When the KCl has melted, the silica transfer tube carrying the helium gas is lowered into the melt. Simultaneously, the helium gas is diverted to bubble through liquid CCl_4. Hence, CCl_4 vapors come into direct contact with the molten KCl, and the bubbling action of the carrier gas insures good mixing. After the RAP treatment, the tube is pulled from the melt, and helium gas without CCl_4 vapor is allowed to flow through the system until the KCl has cooled to room temperature. The KCl is held in the liquid state for about 15 minutes following the RAP treatment to cause some of the residual reaction products to be carried off by the flowing helium. After the processed KCl has cooled to room temperature, the crucible and KCl are removed, and the solidified boule of KCl, which slips freely from the crucible, is sealed in plastic for later use. The KCl boule often has a small, slightly yellow core which is probably trapped Cl_2 gas.

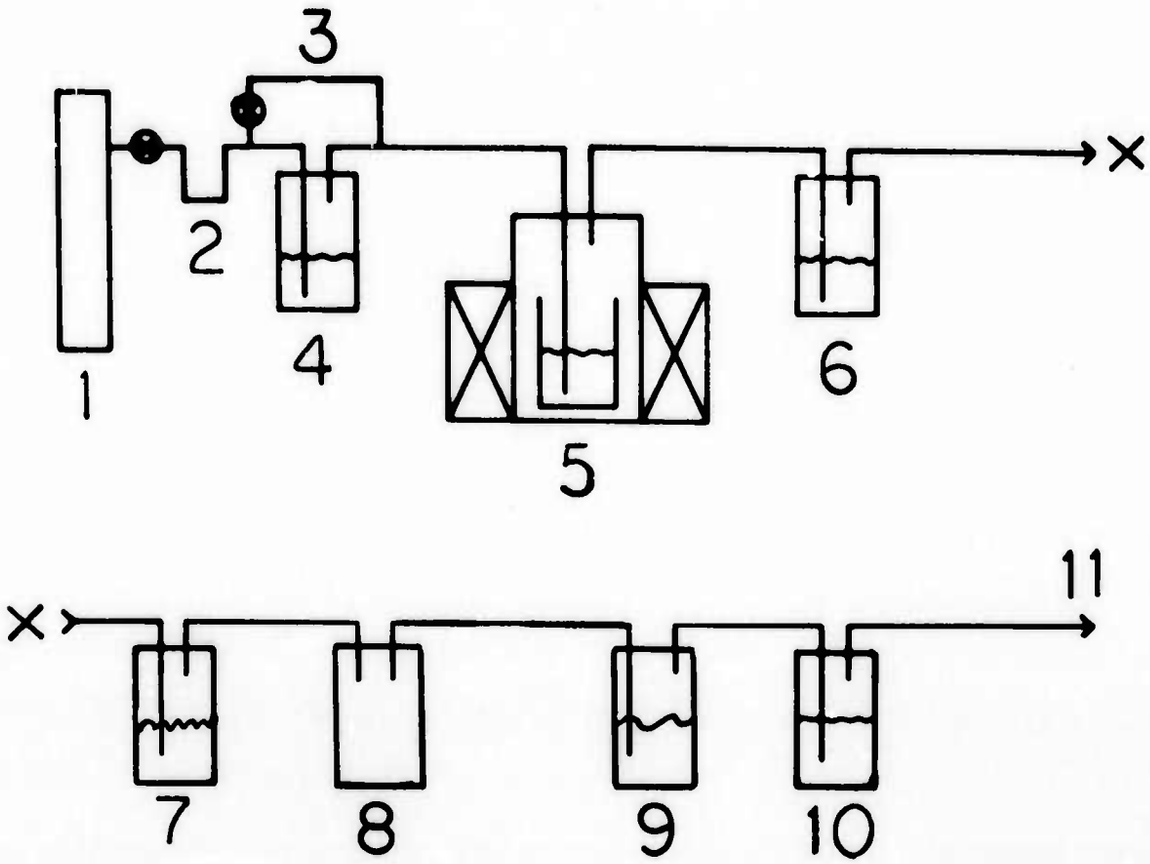

Figure 3. Block Diagram of RAP Apparatus

1. Helium
2. Drying tube
3. Carbon tetrachloride by-pass
4. Carbon tetrachloride
5. Furnace and reaction chamber
6. Empty container
7. Potassium hydroxide (1N)
8. Empty container
9. Ethyl alcohol
10. Water
11. Exhaust

RAP-Bridgman System.

A conventional RAP-Bridgman system has been completed and placed in operation during this quarter. The system is similar to the one described by Klein[5] and is shown schematically in Figure 4. Our current growth procedure is as follows. The viterous carbon crucible is filled with Baker Analyzed KCl powder which has been stored at 150°C and then placed in the Mullite tube growth chamber. The growth chamber is purged with Ar for two hours and then the CCl_4 bubbling is started for the growth run at a rate of 10-12 bubbles/minute. During the week long run this flow rate uses about 10 cm^3 of CCl_4. The temperature of the furnace is then raised to 300°C and the furnace is raised at 15 mm/hr to mix the gas with the melt. The cycle is repeated at 600°C. After the 600°C cycle is completed the furnace temperature is raised to 900°C to melt the KCl and the growth run is started at a furnace lift rate of either 1.5 mm/hr or 0.75 mm/hr. After completion of the 15 cm growth run, the furnace is programmed down to room temperature. The crystals, which often have a few bubbles on their surface slip freely from the crucible.

D. Results

1. Optical Characterization

A number of KCl crystals have been grown by pulling from melts of RAP-Pretreated, RAP-Bridgman grown and untreated reagent grade starting material, and of HCl/Cl_2 treated material purchased from the University of Utah. KCl and NaCl crystals have also been grown by the RAP-Bridgman process. For CO_2 laser window applications the 10.6μm absorption coefficient, $\beta_{10.6}$, is the most important characterization. H. Lipson and P. Ligor at Air Force Cambridge Research Laboratories, M. Hass at Naval Research Laboratories and J. Harrington

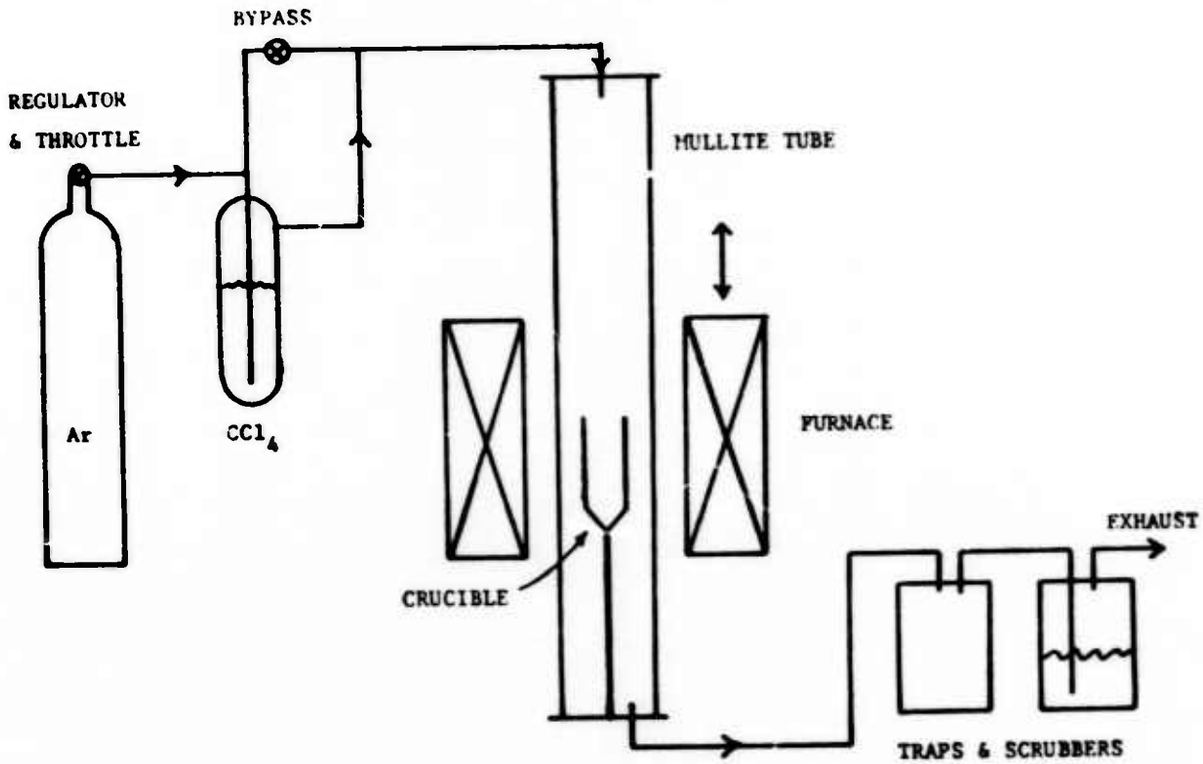

Figure 4. RAP-Bridgman KCl Growth System.

at University of Alabama - Huntsville have calorimetrically measured $\beta_{10.6}$ for a number of our crystals. For the calorimetric measurement, the crystal boule ends were water polished flat and rinsed with isopropyl alcohol. Then the boule was soaked in concentrated HCl and rinsed in acetone. A second, more easily determined, characteristic is the hydroxyl content, C_{OH}. C_{OH}, in μg, OH^- per g KCl, was found from the 204 nm optical absorption band using the relation[7] where β is the peak absorption coefficient in cm^{-1}. The con-

$$C_{OH} = 0.57\beta$$

centration in molar ppm can be found by changing the constant to 2.5. This characterization has a sensitivity of 0.01 to 0.02μg OH/g KCl in a 5 cm long crystal. Dopants such as Sr^{++} tend to obscure the OH band. Table I gives C_{OH} and $\beta_{10.6}$ for a number of our KCl crystals.

TABLE I. KCl CRYSTAL CHARACTERISTICS

Boule	Type	C_{OH}(μg/g)	$\beta_{10.6}$($10^{-4}cm^{-1}$)	Starting Material
022873	Pulled	0.5	42	untreatment
111373	Pulled	0.03	28	RAP-Pretreatment (3/4 hr)[a]
022374	Pulled	--	16	RAP-Pretreatment (3 hr)[a]
021875	Pulled[b]	<0.02	7.4	RAP-Pretreatment (3 hr)[a]
100374	Pulled[b]	--	5.1	RAP-Bridgman
112073	Pulled	0.02	10	UTAH
052074	Bridgman	≥1	--	untreated
062074	RAP-Bridgman	<0.02	4.4	untreated
071874	RAP-Bridgman	--	6.2	untreated
093074	RAP-Bridgman	--	6.8	Sr doped

a. Elapsed time for the RAP-Pretreatment process.

b. Ti gettered atmosphere.

KCl crystals grown from untreated reagent grade start material, such as boule 022873, show both a high OH content and a large $\beta_{10.6}$. This result indicates that starting material should be treated to remove OH and other oxygen related impurities which are thought to contribute to the 10.6μm absorption. The RAP-Bridgman crystal growth process, described above, is the simplest treatment process. It consistently yields crystals with low OH content and $\beta_{10.6}$ values around $5 \times 10^{-4} cm^{-1}$ range. These RAP-Bridgman crystals also show the characteristic Pb band at 272 nm, from which an estimated Pb concentration of 0.5μg Pb/g KCl is obtained. The end pieces of several boules have been cleaved to test for grain boundaries. They do not cleave as readily as pulled crystals and the cleavage planes usually show several small angle variations. We estimate the grain size to be 1 to 10mm.

The RAP-Pretreatment Process was set up to purify starting material for use in the crystal pullers. Initial results were not encouraging since a 3 hour treatment only lowered $\beta_{10.6}$ to 16×10^{-4} (Boule 022374). However, the crystals did show a large improvement in OH content. A Ti gettering furnace was added to purify the Ar gas used as the atmosphere in the sealed crystal pulling systems. Once this was done $\beta_{10.6}$ dropped to values similar to those of the Bridgman grown crystals. KCl Boule 100374 which was pulled in a Ti gettered Ar atmosphere from a RAP-Bridgman grown crystal showed a $\beta_{10.6}$ of $5.1 \times 10^{-4} cm^{-1}$ while boule 021875 which was pulled from a RAP-Pretreated ingot has a $\beta_{10.6}$ of $7.4 \times 10^{-4} cm^{-1}$. We conclude that low absorption KCl can be obtained by pulling from previously purified melts if a gettered inert gas atmosphere is used in a sealed puller. We also conclude that either the RAP-Bridgman or the pretreatment process can be used to purify the starting material. The pretreatment process is somewhat faster since

it can be completed in one 8 hour day. Our pulled KCl crystals do not show the 272 nm Pb band that appears in the Bridgman grown crystals.

2. Doped Crystals

A set of Sr doped and Eu doped KCl crystals were grown for mechanical properties measurements which will be described later in this report.

KCl:Sr crystals were initially pulled from untreated reagent grade KCl melts using anhydrous $SrCl_2$ as the dopant. Later, KCl:Sr crystals were pulled from RAP-pretreated melts. The Sr content of crystals was determined by atomic absorption spectroscopy. Figure 5 gives the molar Sr concentration for the top and bottom of the crystal boule versus the melt concentration. Because of impurity banding and other effects, the reported concentrations are probably not good to better than 25-50% even though the individual analyses are much more reliable than this. The effective segregation coefficient for Sr in KCl, using this apparatus is seen to lie between 0.1 and 0.2. This is in agreement with values found earlier by Kelting and Witt[8] and by Sibley and Russell[9].

Since Eu^{2+} has been shown to strengthen forged KCl[10], we have grown a number of KCl:Eu crystals for our own mechanical studies on single crystals and for forging studies at AFCRL. Eu doped starting material for the crystal puller was prepared by growing a RAP-Bridgman ingot doped with the appropriate amount of $EuCl_3$. Electron paramagnetic resonance measurements on our crystals show that the Eu goes into the KCl lattice as Eu^{++} in a K^+ site with an adjacent K^+ vacancy.[11] The Eu^{++} also has two strong absorption bands in the u.v. as shown in Fig. 6. The position of the peaks are in good agreement with the results of Mehra.[12] The dashed and solid curves in Fig. 6 are for the top and bottom sections of the pulled boule. When calibrated, absorption bands can be used to determine the Eu concentration in the crystal. We have

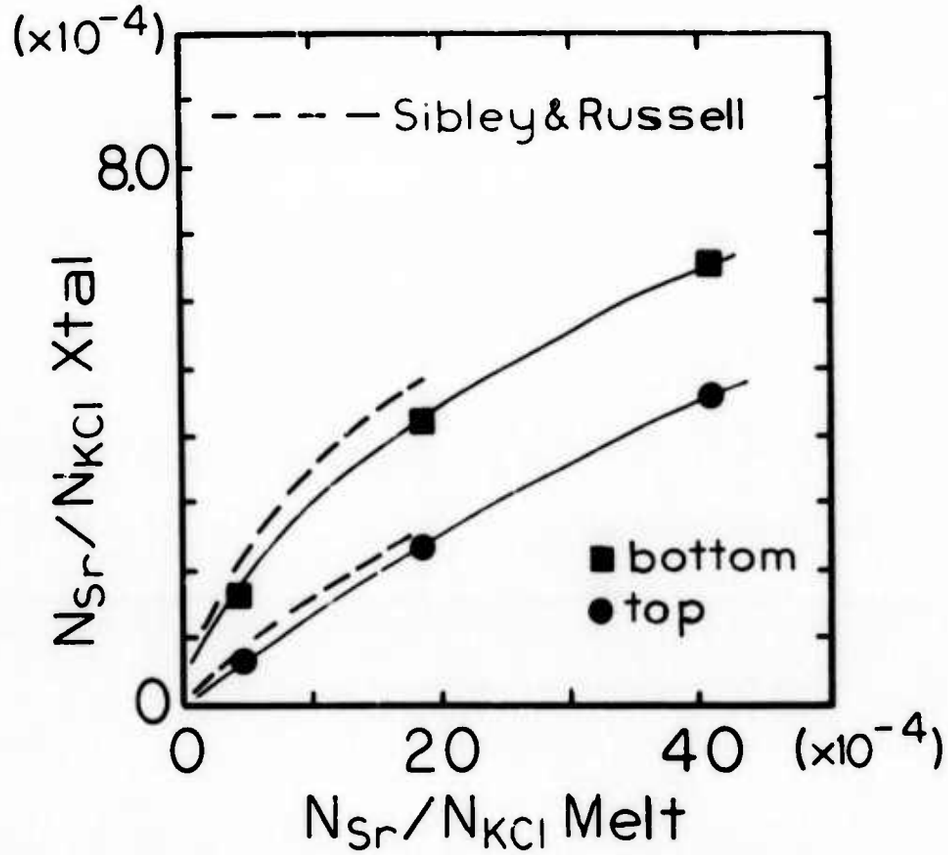

Figure 5. Crystal Sr Content Versus Melt Sr Content

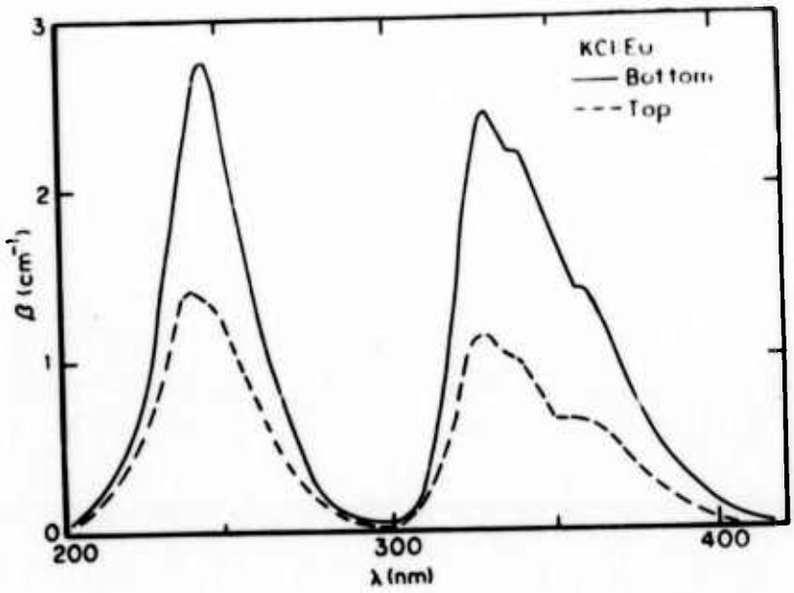

Figure 6. The Eu^{++} absorption bands are shown. The solid curve is for a sample taken from the bottom of the pulled boule while the dashed curve is for a sample taken from the seed end.

measured the peak absorption coefficient of the 243 nm Eu^{++} band in KCl for a number of different samples and then used atomic absorption spectroscopy to directly determine the Eu concentration. Fig. 7 shows the Eu concentration in molar ppm versus the peak absorption coefficient. With this calibration the Eu concentration can be determined by measuring the optical absorption. We find that

$$C_{Eu} = 17.2\ \beta$$

where C is the Eu^{++} concentration in molar ppm and β is the 243 nm band peak absorption coefficient in cm^{-1}. The authors would like to thank Prof. Zuhair Al-Shaieb of the OSU Geology Dept. for his help with the atomic absorption analyses. The mechanical properties of both KCl:Sr and KCl:Eu will be discussed later in this report.

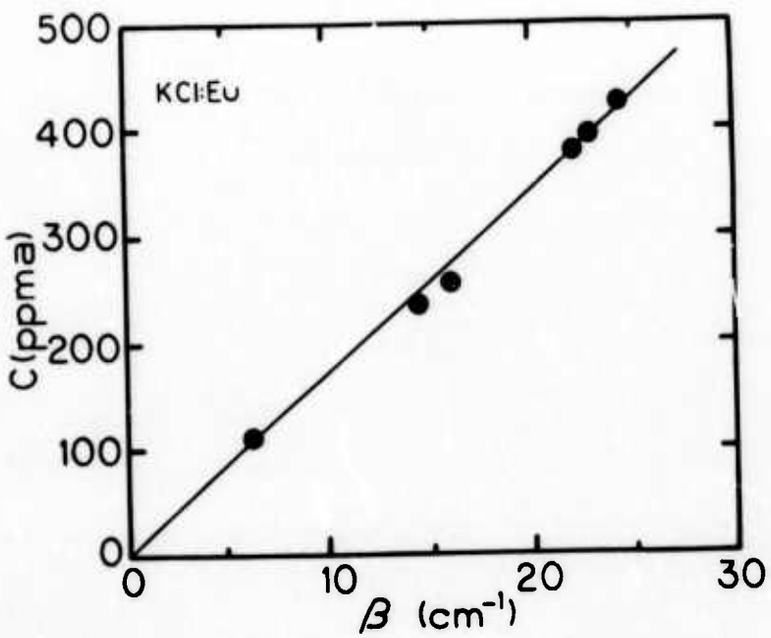

Figure 7. The Eu content in atomic ppm determined by atomic absorption spectroscopy is plotted against the peak absorption coefficient for the 243 nm Eu^{++} band in KCl.

E. References

1. F. Rosenberger, Mat. Res. Bull. 1, 55 (1966).

2. C. T. Butler et al., J. Chem. Phys. 45, 968 (1966).

3. C. T. Butler et al., "A Method for Purification and Growth of KCl Single Crystals," ORNL Report, ORNL-3906, Feb., 1966.

4. R. C. Pastor and A. C. Pastor, Mat. Res. Bull. 10, 251 (1975).

5. P. H. Klein, NRL, SemiAnnual Technical Report, ARPA Order 2031, June, 1973.

6. F. Rosenberger, "Purification of Alkali Halides," in Ultrapurity, M. Zief and R. Speights, eds. Marcel Dekker, Inc. N.Y., 1972.

7. B. Fritz, F. Lüty and J. Anger, Z. Phys. 174, 240 (1963).

8. H. Kelting and H. Witt, Z. Physik 126, 697 (1949).

9. W. A. Sibley and J. R. Russell, J. Appl. Phys. 36, 810 (1965).

10. E. F. Shrader, Harshaw, AFML-TR-74-165.

11. M. Young and L. E. Halliburton, Oklahoma State University, private communication, 1975.

12. K. Mehra, J. Opt. Soc. Am. 58, 853 (1968).

III. THE EFFECT OF IONIZING RADIATION ON THE 10.6μm ABSORPTION OF KCl AND NaCl

A major part of this project has been an investigation of the effects of radiation damage on the 10.6μm absorption of alkali halide laser window materials. This work which was carried out jointly with H. Lipson and P. Ligor at the Air Force Cambridge Research Laboratories is described below in a draft of a joint paper to be submitted to the Journal of Applied Physics.

THE EFFECT OF IONIZING RADIATION ON THE 10.6 μm ABSORPTION OF KCl AND NaCl

H. G. Lipson and P. Ligor
Air Force Cambridge Research Laboratories (AFSC)
Hanscom AFB, Bedford, MA 01731

and

J. J. Martin*
Department of Physics
Oklahoma State University
Stillwater, OK 74074

ABSTRACT

The optical absorption of both KCl and NaCl as measured by CO_2 laser calorimetry has been found to increase upon irradiation with ^{60}Co gammas. The absorption is found to increase faster than the first power of the F center density in both materials. An additional low intensity gamma irradiation of a KCl sample which broke up the F aggregate centers without increasing the total damage lowered the 10.6 μm absorption. A subsequent bleaching of the sample partially restored the absorption. Additively colored KCl showed a comparable 10.6 μm absorption. Therefore, the 10.6 μm absorption increase is caused by the F aggregate bands rather than by the Cl^0 interstitial clusters. A plot of the 10.6 μm absorption versus the M center density shows a linear dependence for both KCl and NaCl.

---

*Supported by ARPA, monitored by AFCRL.

A. Introduction

Because of their excellent infrared properties KCl and NaCl are possible candidates for high power CO_2 laser window applications. However, their low mechanical strength requires that mechanisms for increasing their strength be found which do not degrade the optical properties. Radiation damage is a well known strengthening mechanism in alkali halides (1,2). While the color centers produced by the radiation damage process have been extensively studied in the near infrared and visible regions there is very little information available on their effects in the CO_2 laser region.

Ionizing radiation damages alkali halides by a photochemical process (3). The process produces negative ion vacancies containing electrons, (F centers) and an equivalent number of halogen interstitials in large clusters (4). It is the halogen interstitial clusters rather than the F centers that increase the strength of the crystal (1,5). The optical properties of F and F aggregate centers have been reviewed by Fowler (6) and by Compton and Rabin (7). Neither the F nor the F aggregate bands have been observed by the usual spectrophotometry methods to extend into the 10 μm region. However, the increased sensitivity of laser calorimetry makes possible the observation of radiation induced absorption at the CO_2 laser wavelength (8). An absorption increase at 10.6 μm upon irradiation might come from the halogen interstitial clusters, long wavelength tails of the F and F aggregate bands, low lying forbidden transitions of the aggregate centers such as the ground state singlet to ground state triplet of the M center (9) or aggregate centers formed by next nearest neighbor F centers (10). We report here CO_2 laser calorimetric absorption measurement on undoped KCl and NaCl as a function of radiation damage. Magee et al. (11) have reported similar results for mixed KCl crystals.

B. Experimental Procedure

The KCl and NaCl crystals for this study were grown at Oklahoma State University by the RAP-Bridgman process (12) from reagent grade powder. This growth technique typically yields KCl crystals with absorption coefficients in the low $10^{-4}cm^{-1}$ at 10.6 μm. The samples for the 10.6 μm laser calorimetric measurements were cut from the boules with a H_2O carrying wire saw, water polished and then chemically polished with concentrated HCl (13) immediately preceding the measurement. The initial absorption values at 10.6 μm for samples KCl-I and KCl-II were 4.0×10^{-4} and 6.3×10^{-4} cm^{-1} respectively. The NaCl sample had an absorption of 10.2×10^{-4}/cm which is near the intrinsic limit. A number of thin (1 mm x 5 mm x 5 mm) wafers were cleaved from the remainder of each boule and used as dosimetry test pieces for the irradiation experiments.

The calorimetry and dosimetry samples were simultaneously irradiated at approximately 40°C in the AFCRL 1MR/hr ^{60}Co gamma source. After each irradiation the calorimetry sample was repolished in concentrated HCl. The absorption coefficient at 10.6 μm was measured with standard laser calorimetry methods (14,15). F and M center peak absorption coefficients were determined from visible and near infrared optical scans on the thin dosimetry samples with a Cary 14 spectrophotometer. Occasional scans on the thick (2cm) calorimetry samples showed reasonable agreement with the dosimetry samples in the low absorption ranges.

C. Results and Discussion

Figure 1 shows the growth of the 10.6 μm absorption coefficient, $\beta_{10.6}$, for both KCl and NaCl as a function of ^{60}Co gamma irradiation. $\beta_{10.6}$ appears

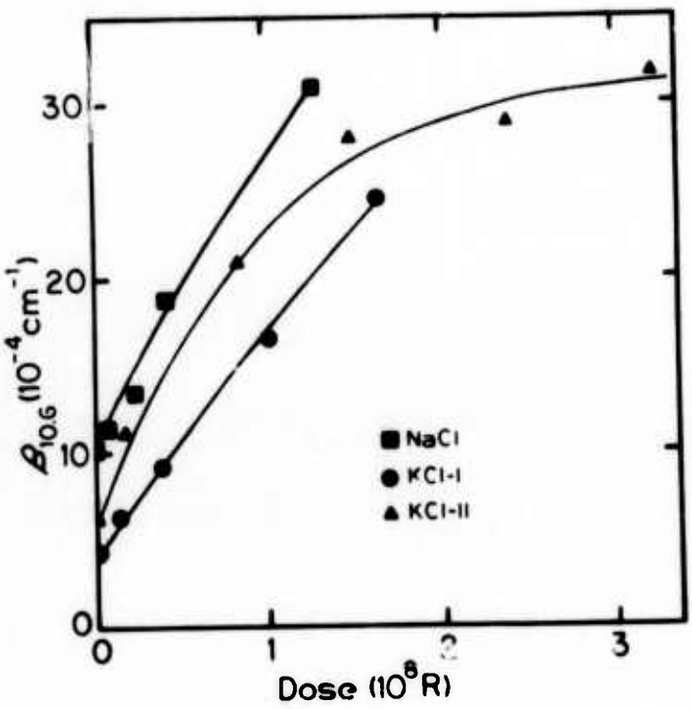

Figure 1. The 10.6 μm absorption coefficients, $\beta_{10.6}$, for a NaCl sample and two KCl samples are shown as a function of ^{60}Co gamma irradiation. The dose rate was approximately 10^6 R/hr.

to saturate for the higher doses. Figure 2 shows the spectra observed in one of the small KCl dosimetry samples. The F band absorption coefficients, β_F, for each calorimetry test which were spectrophotometrically measured on the small test samples are shown as a function dose in Figure 3. In order to determine the amount of radiation damage in each sample the number of F centers, per cm^3, n_F, was calculated from Smakula's equation

$$n_F f = 0.87 \times 10^{17} \frac{n}{(n^2 + 2)^2} \beta_F W$$

where f is the oscillator strength, n is the index of refraction, β_F is the peak F band absorption coefficient, in cm^{-1}, and W is the width of the F band at half maximum, in eV. (6) We have used an oscillator strength of 0.7 for the F center. Figure 4 shows that $\beta_{10.6}$ increases much more rapidly as a function of the total damage, as measured by n_F, for KCl than for NaCl. Since the Cl^o interstitials and the color centers are produced in equal numbers, Figure 4 suggests that the increase in $\beta_{10.6}$ upon irradiation is caused by the F and F aggregate centers rather than by the interstitials.

Since additive coloration produces F and F aggregate centers without interstitials the above conclusion can be confirmed by measuring $\beta_{10.6}$ for an additively colored sample. Three wafers (3 cm dia x 0.5 cm) were cut and polished from KCl sample III. The control wafer, A, had a $\beta_{10.6}$ of $8 \times 10^{-4} cm^{-1}$; the slightly high $\beta_{10.6}$ may be due to the unusual sample geometry. Wafer C was heated in the presence of K vapor to 650°C and then slowly cooled. An optical scan showed for this additively colored sample, $\beta_F = 80\ cm^{-1}$. Wafer B was irradiated with 1.5 MeV electrons until it had approximately the same β_F. The $\beta_{10.6}$ values were $80 \times 10^{-4} cm^{-1}$ and $120 \times 10^{-4} cm^{-1}$ for

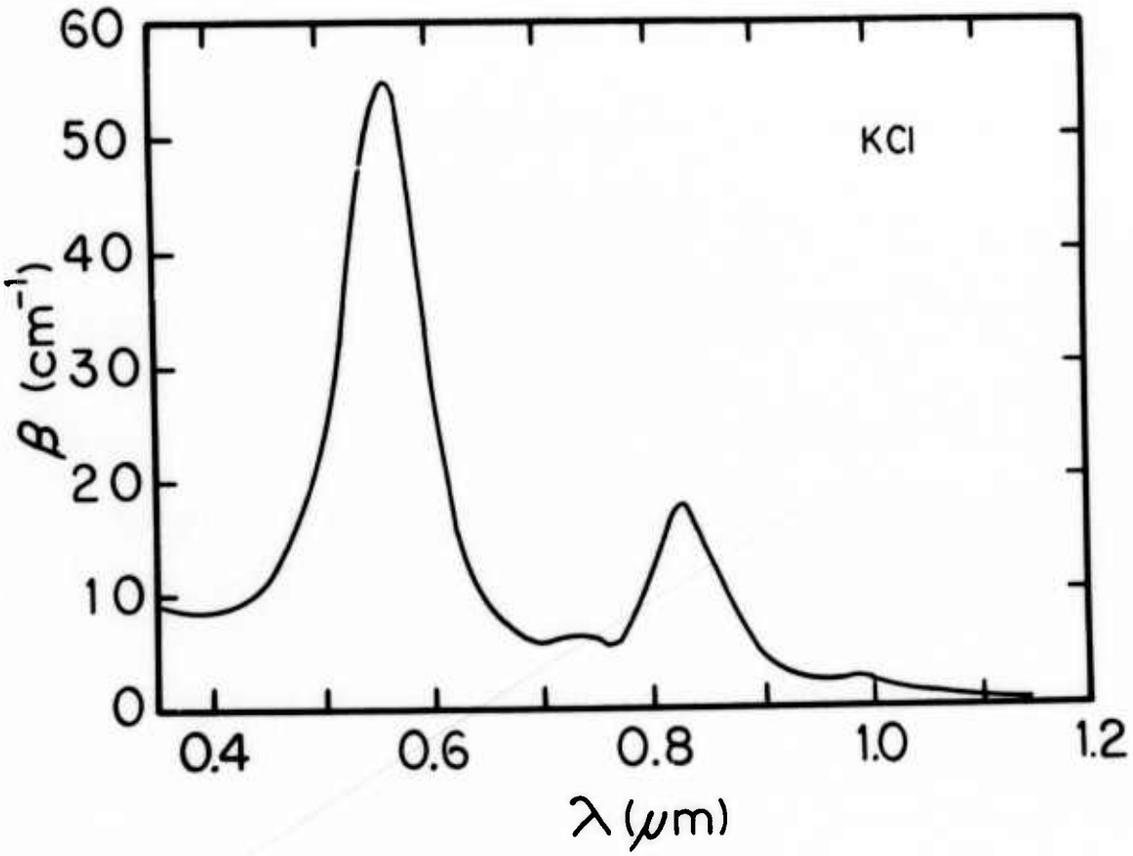

Figure 2. The absorption spectrum of one of the KCl dosimetry samples is shown. The spectrum shows that the R and N center densities are much smaller than the F and M densities in our "as irradiated" samples.

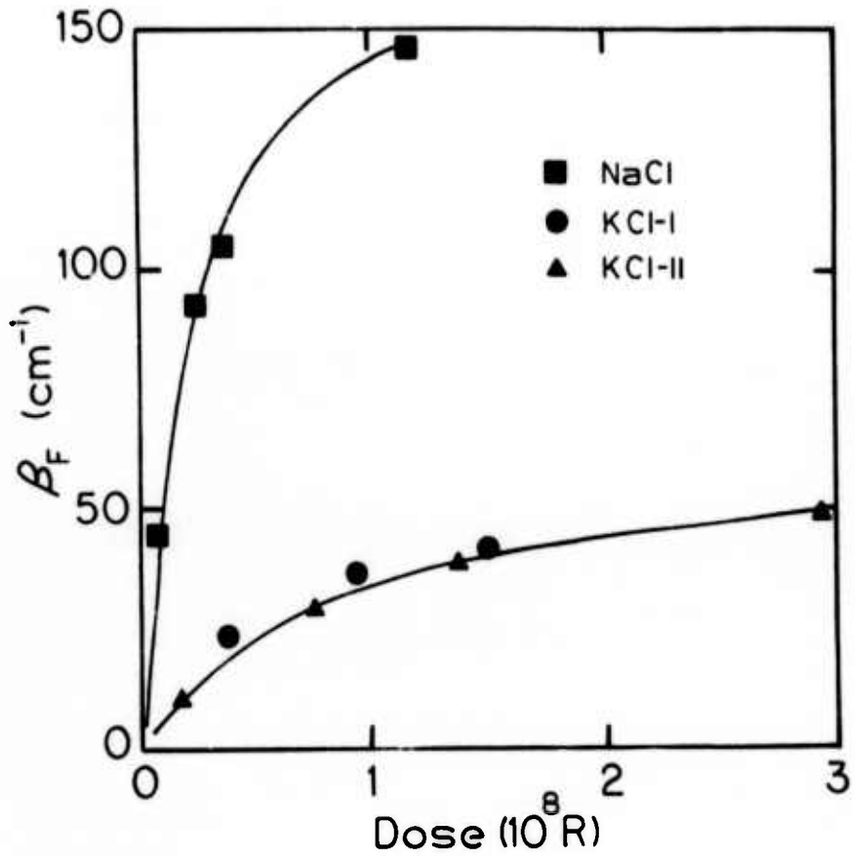

Figure 3. The peak F band absorption coefficient for the NaCl sample and two KCl samples is shown as a function of ^{60}Co gamma irradiation.

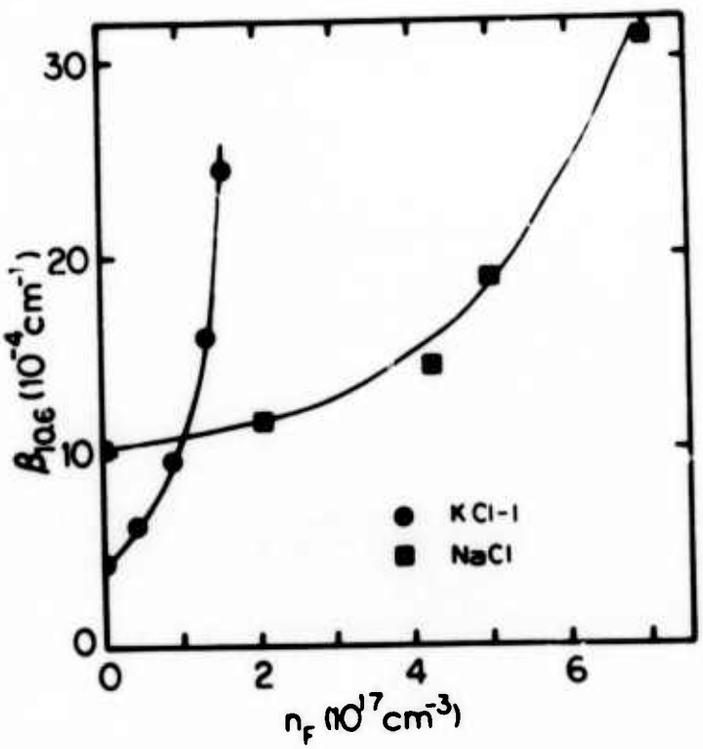

Figure 4. $\beta_{10.6}$ is shown as a function of the F center density, n_F, for both NaCl and KCl irradiated with ^{60}Co gammas. Although both NaCl and KCl show a $\beta_{10.6}$ that increases faster than the first power of n_F upon irradiation, the $\beta_{10.6}$ increase is much less in NaCl than KCl for equivalent F center densities.

The additively colored and electron irradiated samples respectively. The large $\beta_{10.6}$ increase for the additively colored sample shows that the 10.6 μm absorption is caused by F aggregate centers rather than by the Cl^{o} interstitials which are not present in this sample.

Figure 4 also shows that $\beta_{10.6}$ increases faster than the first power of the F center concentration. Since the M center density, n_M is known to grow as the square of the F center density (7) we have plotted $\beta_{10.6}$ as a function n_M in Figure 5. n_M was calculated from the measured M band 8×10^{-4} cm^{-1} absorption coefficient. A short low intensity ($<3 \times 10^4$ R/hr) ^{60}Co gamma irradiation was used to break up the F aggregate centers in sample KCl-I. This treatment which would not significantly increase the total damage lowered $\beta_{10.6}$ from 24.5×10^{-4} to $8 \times 10^{-4} cm^{-1}$. An optical scan on the calorimetry sample produced the spectrum shown by the solid line in Fig. 6. The measured $\beta_{10.6}$ value is in reasonable agreement for this M center density when compared with the $\beta_{10.6}$ versus n_M curve in Fig. 5. The sample was then given a 23 hr bleach with an unfiltered Hg lamp. The bleach enhanced the F aggregate bands as shown by the dashed curve in Fig. 6 (the M band was saturated for the 2 cm thick sample) and raised $\beta_{10.6}$ to $14 \times 10^{-4} cm^{-1}$.

These results show that the increase in $\beta_{10.6}$ of both KCl and NaCl upon irradiation is caused by the F aggregate bands. The 10.6 μm absorption appears to increase proportional to the M center density for both pure KCl and NaCl. Magee et al. (11) have reported that the $\beta_{10.6}$ increase that they observed in KCl crystals doped with Rb, Br or Eu irradiated with 1 MeV electrons at a rate of 3.3×10^5 R/sec seems to be more closely related to the R center than to either the F or the M center. Of course the dopants and the much more intense irradiation may alter aggregate center population. As shown in Fig. 2 our

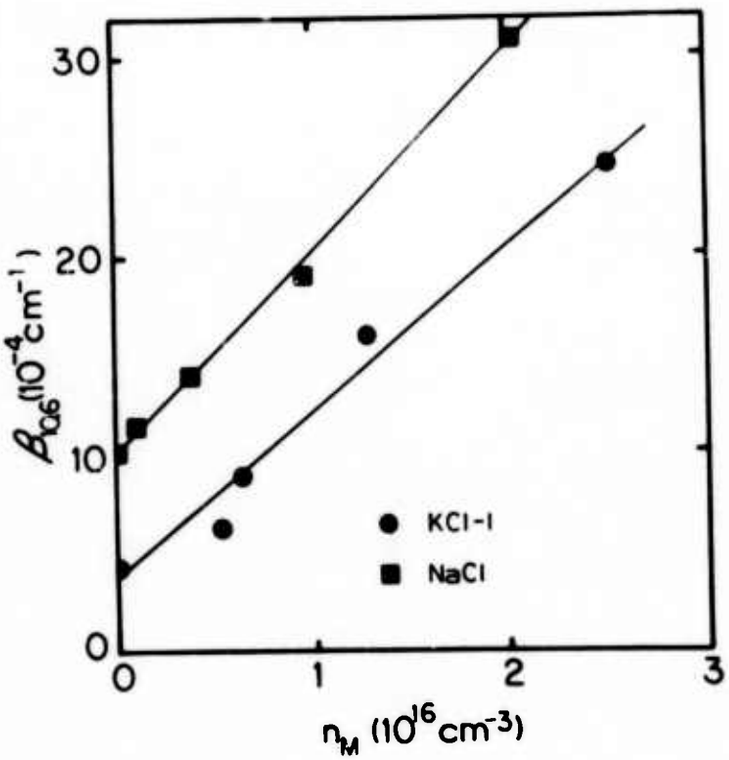

Figure 5. $\beta_{10.6}$ is seen to increase linearly with the M center density, n_M, in both NaCl and KCl.

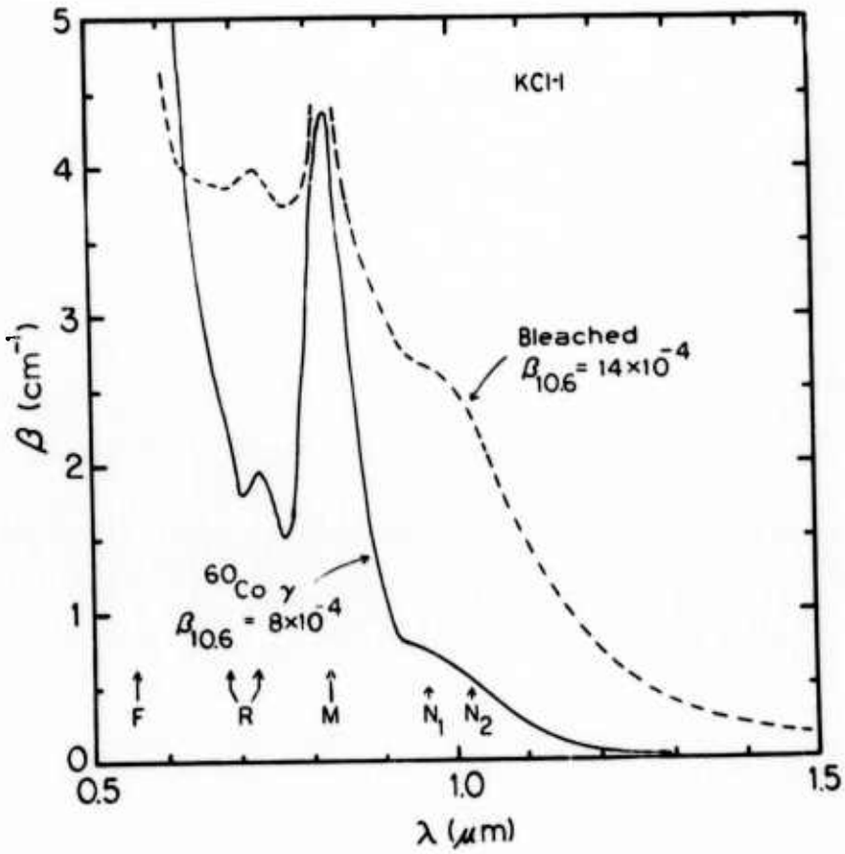

Figure 6. The solid curve shows the absorption spectrum of calorimetry sample KCl-1 after it was given a short low intensity gamma irradiation to break up the F aggregate bands. $\beta_{10.6}$ was lowered from 24.5 x 10^{-4} cm^{-1} to 8 x 10^{-4} cm^{-1} by this process. The dashed curve shows the spectrum after the sample was bleached with a Hg lamp. The M band saturated the spectrophotometer and $\beta_{10.6}$ rose to 14 x 10^{-4} cm^{-1}.

samples show only very small R and N bands. We can, however, conclude that the absorption increase is caused by the F aggregate centers.

The 10.6 μm absorption increase may be caused by tails of the aggregate bands, by low lying transitions associated with the conventional aggregate centers or by other types of aggregate centers. If the M band has a Gaussian shape as reported by Boettler and Compton (16) then it would not be strong enough in the 10 μm region to cause the observed absorption. A Lorentzian line shape would be strong enough. However, the same absorption increase is observed in both KCl and NaCl. If the increase were caused by a tail of the M band (or related center) it should be less in NaCl than in KCl since the F aggregate centers have moved towards the visible. Thus, it seems more likely that the absorption is caused by low lying transitions associated with the F aggregate centers.

If the absorption is directly related to the M center it should be possible to observe a polarization dependence if a sample is prepared with oriented M centers. An oriented single crystal KCl sample was irradiated and then bleached with F band light propagating in the [001] direction and polarized in the [110] direction so as to produce [110] oriented M centers. Fig. 7a shows the M band spectrum measured with light polarized in either the [110] or the $[1\bar{1}0]$. Figure 7b shows that about 10% of the centers were oriented preferentially in the [110] direction. The 10.6 μm absorption coefficient was also measured with the laser beam polarized first in the [110] and then in the $[1\bar{1}0]$ direction. The results were $\beta_{[110]} = (3.96 \pm 0.11) \times 10^{-4} cm^{-1}$ and $\beta_{[1\bar{1}0]} = (3.78 \pm 0.06) \times 10^{-4} cm^{-1}$. The change in the absorption is approximately one half of the amount predicted by the 10% M center orientation. The result is consistent with at least part of the absorption increase coming from the M center. If the 10.6 μm absorption increase is directly

related to the M center it perhaps comes from the normally forbidden ground state singlet to ground state triplet transition (9,17). The other F aggregate centers also have similar low lying states which may contribute. Alternatively, as suggested by Lüty (10), other types of aggregate centers, such as two F centers separated by one or more atomic sites, may also contribute to the 10.6 μm absorption.

CONCLUSIONS

Radiation damage causes the 10.6 μm absorption of both KCl and NaCl to increase. The absorption increase is caused by the F aggregate centers rather than by the Cl^{o} interstitials. For the radiation intensities used for these experiments the absorption increase is directly proportional to the M center density for both KCl and NaCl. It is probably caused by low lying transitions of F aggregate centers.

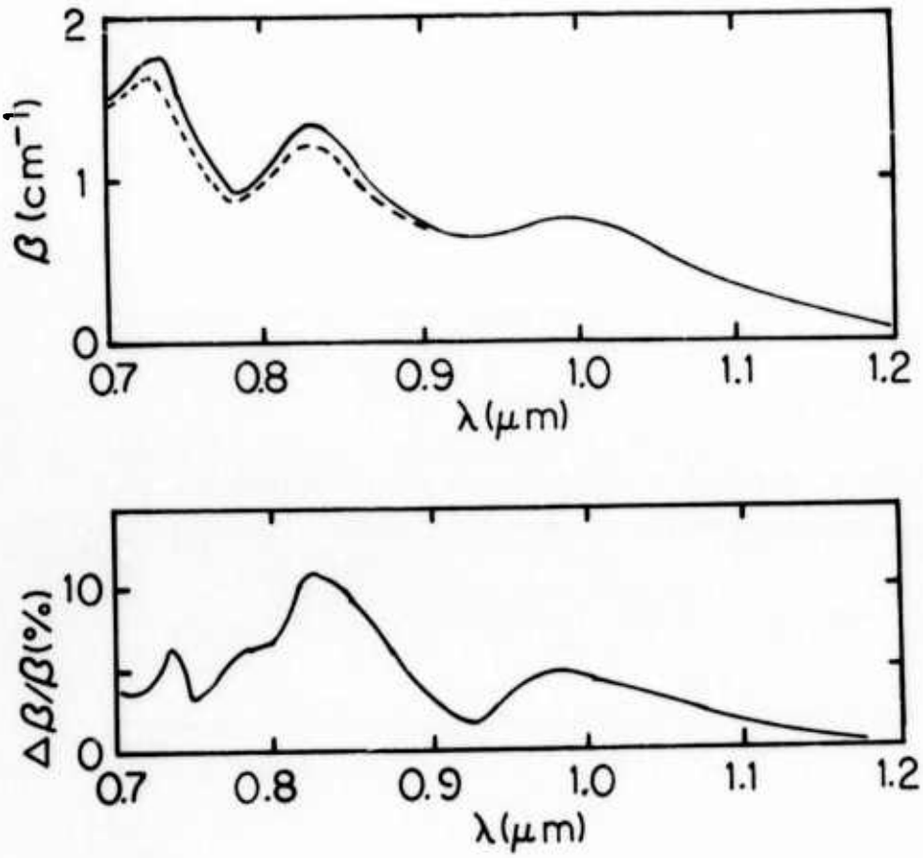

Figure 7. The solid curve in the upper figure shows the absorption spectrum of a KCl sample bleached with F band polarized in the [110] direction propagating in the [001] direction measured with light also polarized in the [110] direction. The dashed curve shows the spectrum measured with [1$\bar{1}$0] light. The lower figure gives the degree of polarization and shows that approximately 10% of the M centers were oriented.

D. References

1. J. S. Nadeau, J. Appl. Phys. 34, 2248 (1963).

2. W. A. Sibley and E. Sonder, J. Appl. Phys. 34, 2366 (1963).

3. E. Sonder and W. A. Sibley, In Point Defects in Solids, J. H. Crawford and L. Slifkin, eds., Plenum Press, 1972.

4. L. W. Hobbs, A. E. Hughes and D. Pooley, Proc. R. Soc. London, A332, 167 (1973).

5. J. R. Hopkins, Phys. Stat. Sol. (a), K 15 (1973).

6. W. Beal Fowler, in Physics of Color Centers, W. Beal Fowler, ed. Academic Press, N.Y., 1968.

7. W. D. Compton and H. Rabin, Solid State Physics 16, 121 (1964).

8. H. G. Lipson, P. Ligor, A. Kahan and J. J. Martin, B 11. A.P.S., 20, 377 (1975).

9. Ref. 6, p. 113.

10. Lüty.

11. T. J. Magee, N. Johnson and J. Peng, Phys. Stat. Sol. a) 29, (to be published).

12. R. C. Pastor and A. C. Pastor, Mat. Res. Bull. 10, 251 (1975).

13. J. W. Davisson, J. Mat. Sci. 9, 1701 (1974).

14. H. G. Lipson, L. H. Skolnik and D. L. Stierwalt, in Proc. Third Conf. on High Power Laser Window Materials, C. A. Pitha and B. Bendow, eds. U. S. Air Force Cambridge Research Laboratories Tech Report TR-74-0085(1) Bedford, Mass. (1974), p. 337.

15. L. H. Skolnik, A. Hordvik and A. Kahan, Appl. Phys. Letters 23, 477 (1973).

16. J. L. Boettler and W. D. Compton, Phys. Rev. 173, 844 (1968).

17. H. Engstrom, Phys. Rev. B 11, 1689 (1975).

IV. MECHANICAL PROPERTIES

A. Introduction

Because of its low infrared optical absorption, KCl is a prime candidate for CO_2 laser windows. However, window applications require material with greater mechanical strength than that possessed by monocrystalline KCl; hence, it is desirable to develop techniques which increase the yield strength, τ_e $\simeq$2 MN/m^2, while maintaining a low infrared absorption. Promising strengthening mechanisms include: monovalent solid-solution hardening, $\tau_{e_{max}} \simeq$20 MN/m^2 (1); grain boundary hardening, $\tau_{e_{max}} \simeq$30 MN/m^2 (2,3), and tetragonal defect hardening, $\tau_{e_{max}} \simeq$10 MN/m^2 (4).

Fleischer (5) has shown that the interaction between dislocations moving along the slip plane and isolated defects increases the resolved flow stress, τr. This increase can be expressed as

$$\Delta\tau_r = \frac{G}{n} C^{\frac{1}{2}} \qquad (1)$$

where G is the shear modules for the slip system, C is the mole fraction defect concentration, and n is a number which depicts the hardening effectiveness for the particular type of defect. Fleischer found approximate n values of 10 and 100 for interstitials and divaconcies, respectively. The $C^{\frac{1}{2}}$ dependence will only be observed if the moving dislocation samples isolated on individual defects. We describe below the tetragonal defect strengthening of alkali halide window materials. Section B discusses the effects of ionizing radiation on the strength of KBr_xCl_{1-x} mixed crystals and on press forged KCl. Section C discusses the effects of Sr^{2+} and Eu^{2+} dopants on the strength of single crystal KCl. Since the temperature dependence of the strength may also be an important parameter for laser window design we have investigated the strength of KBr_xCl_{1-x} mixed crystals and of KCl:Sr crystals as a function of temperature. Those results

are reported in section D. The relationship between flow stress, Vickers Hardness and dislocation motion has been reported in detail elsewhere (6) for KCl and KBr_xCl_{1-x} mixed crystals.

B. The Effects of Ionizing Radiation on the Flow Stress of KCl_xBr_{1-x} Mixed Crystals and of Forged KCl.

Early radiation hardening studies of a number of alkali halides (7,8,9) show a $C^{\frac{1}{2}}$ dependence of the flow stress on F center concentration. However, the F centers alone are not the cause of the change in flow stress (9,10). The strengthening of the irradiated alkali halides is due to the halogen interstitials produced in the radiation damage process.

Recent electron microscope studies of irradiated alkali halide foils by Hobbs, Hughes, and Pooley (11) indicate that interstitials produced during room temperature irradiation either externally with 400 keV electrons or in the 100 keV microscope beam cluster as prismatic dislocation loops. Hence, the hardening is not due to interactions of dislocations and individual interstitials but rather to the interactions of dislocations and interstitial clusters. Their results indicate that the interstitial clusters in KCl are in the form of long needle-like dipole loops which lengthen with increased radiation dosage, the interstitial clusters in KI are rounded and grow radially with increased dosage, and the clusters in KBr are elongated ellipsoids. Hobbs and Howitt (12) have shown theoretically that for the elongated dipole loops in KCl the increase in flow stress is still proportional to $C^{\frac{1}{2}}$:

$$\Delta\tau_r = \frac{Gb}{3k} \frac{2}{(ad)^{\frac{1}{2}}} C^{\frac{1}{2}} \qquad (2)$$

where b, the Burgers vector, equals a/2 [110], k ≈ 4 for the dislocation-dipole loop interactions, a is the lattice constant, and d is the dipole width. For KCl they found that the dipole width remained constant for the radiation doses investigated. For systems which form rounded dislocation

loops, $\Delta\tau_r$ is expected to be proportional to $C^{\frac{1}{4}}$, and Hobbs and Howitt (25) observed this to be the case in KI. The case of KBr should be somewhat intermediate to KCl and KI.

The flow stress for the KBr_xCl_{1-x} alloy system and for forged KCl has been measured as a function of radiation dose. The alloy system measurements should provide information on the hardening by interstitial clusters in the transition region between the long, narrow loops in KCl and the elongated, but wider loops in KBr. Recently, Becher et al. (13) have found that forged $KCl:Sr^{2+}$ samples show significantly greater yield strengths and that the Petch relation

$$\tau = \tau_o + kd^{-\frac{1}{2}} \qquad (3)$$

where τ is the engineering flow stress of the forged sample, τ_o is flow stress of the single crystal, k is a constant and d is the average grain size holds with an increased τ_o. Because of the possibility of a similar "additive" hardening due to radiation damage in forged KCl and because of the possibility that the already deformed material may alter the interstitial cluster formation we have investigated the radiation hardening of "Polytran" polycrystalline KCl from the Harshaw Chemical Company.

Flow stress samples (approximately 1.5mm x 1.5mm x 8mm) and optical test samples (6mm x 6mm x 2mm) were cleaved from the alloy single crystals and sawed from the Polytran KCl ingot. The polycrystalline samples were water and HCl polished. The average grain size was approximately 25 μm, as determined from photomicrographs of the water etched surface. A set of from 6 to 10 flow stress samples and an optical sample were wrapped in Al foil and were irradiated with 1.5 MeV electrons from the O.S.U. Van De Graaff. The flow stress measurements were made under compression on an Instron testing machine.

The engineering flow stress, τe, was taken to be the stress value at the intersection of the tangents to the elastic and first plastic flow portions of the curve. The single crystal samples were compressed along the [100] direction so $\tau_r = \frac{1}{2} \tau e$. The radiation dose was determined by measuring the F center concentration with a Cary 14 spectrophotometer.

The resolved flow stress, τ_r, versus the square root of the molar F center concentration, C, for the KBr_xCl_{1-x} system is shown in Figure 1. The resolved flow stress for all compositions is directly proportional to the square root of the F center concentration. However, in some of the materials, a slight softening was observed for low radiation doses. A similar observation was made by Nadeau (9) for a few of the pure alkali halides. The softening occurs during early stage coloration where few stable interstitials are thought to be produced.

Since the flow stress increases as the square root of the F center concentration for all compositions, the interstitial clusters must retain the elongated shape as x varies from 0 to 1 in the KBr_xCl_{1-x} system. The widths of the clusters may be estimated from Equation 2 and the slopes of the τ_r versus $C^{\frac{1}{2}}$ curves. For the alkali halide's slip system

$$G = [\tfrac{1}{2} C_{44} \quad (C_{11} - C_{12})]^{\frac{1}{2}} \qquad (3)$$

where the C_{aa}'s are the elastic constants. The shear moduli for the mixed alkali halides were calculated from the elastic constants report by Slagel and McKinstry. (19) Table I lists the shear moduli and the estimated cluster widths. The estimated cluster width for KBr is 3 to 4 times that for KCl This is in reasonable agreement with the electron microscope results (11). Since the mixed crystals are probably somewhat inhomogenous, the d's listed

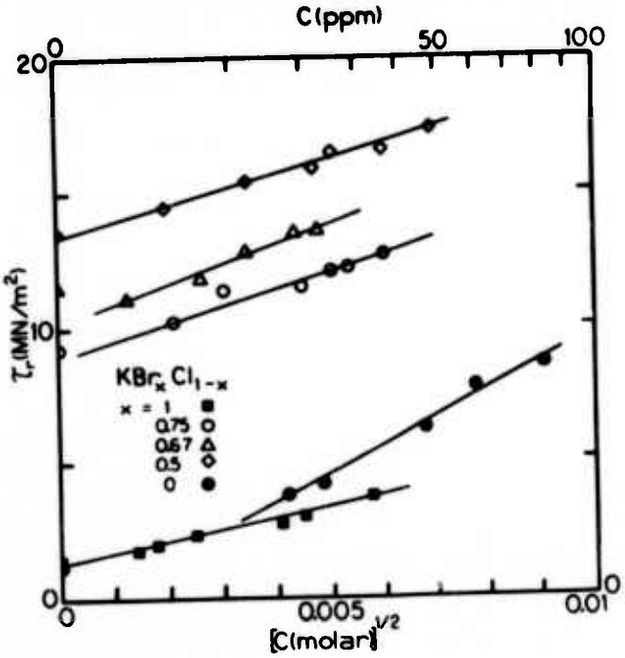

Figure 1. The resolved flow stress, τ_r, is shown as a function of the square root of the molar F center concentration for irradiated KBr_xCl_{1-x} crystals.

TABLE I

Shear Moduli, G, and Cluster Widths, d, for KBr_xCl_{1-x}

x	G(10^3 MN/m^2)	d (Å)
1.0 (KBr)	8.5	18
0.75	8.95	18
0.67	9.13	8
0.5	9.4	11
0.0 (KCl)	10.3	5

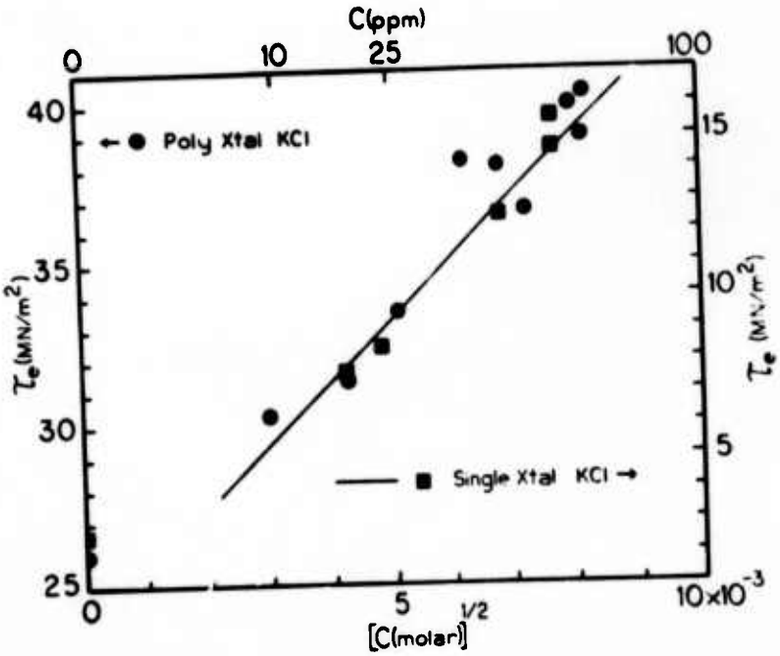

Figure 2. The engineering flow stress for polycrystalline KCl is given on the left hand scale and the engineering flow stress for single crystal KCl is given on the right. Both are shown as a function of the square root of the molar F center concentration.

in Table II are not precise; hence, the fact that there is not a smooth transition from KCl to KBr is understandable. However, the general trend of the data is for decreasing cluster widths as x varies from 1 to 0 (KBr to KCl).

The engineering flow stress, τ_e, versus the square root of the molar F center concentration, C, for irradiated monocrystalline KCl and polycrystalline KCl is shown in Figure 2. These results show that the radiation hardening is independent of the grain boundary hardening, and that the hardening mechanism is not altered by the deformation caused by the forging process. The radiation hardening is additive for the defect concentrations studied. Since the slope of the τ_e versus $C^{\frac{1}{2}}$ curve for polycrystalline KCl is the same as that of the monocrystalline KCl, the widths of the interstitial clusters apparently remain constant and cluster formation is not altered by the polycrystalline nature of the sample. Hobbs, et al. (11) found that the cluster length increased but that the cluster width and density remained constant with increased radiation dose. Their data indicate that the average distance between clusters is $\simeq$ 0.1μm and that, for an F center concentration of $5 \times 10^{17}/cm^3$, the cluster lengths are less than 0.1μm. The fact that our studies demonstrated no grain boundary-interstitial cluster interactions, i.e., that the radiation hardening mechanism was unaltered by the polycrystalline nature of the material, is not surprising, since the average grain size for the measured polycrystalline KCl was 25μm. It would be interesting to investigate the effects of ionizing radiation in polycrystalline materials having average grain size $\simeq$ 1μm to see if grain boundary-interstitial cluster interactions could be observed.

The authors would like to thank the Harshaw Chemical Company for supplying the Polytran KCl material.

The above results show that radiation damage can be effectively used to strengthen alkali halide crystals that have already been strengthened either by alloying with monovalent ions or by forging and that the strengthening is "additive". Unfortunately, at least for CO_2 laser applications, the radiation damage also degrades the 10.6μm absorption.

C. Flow Stress of KCl:Sr and KCl:Eu Single Crystals.

When Sr^{++} and Eu^{++} preferentially enter the KCl lattice substitutionally for a K^+ ion; change neutrality requires the complementary formation of a K^+ vacancy. Dryden et al. (14) have found that in KCl:Sr and other alkali halides doped with alkaline earths that at room temperature the divalent ion and cation vacancy are paired and that these pairs may be aggregated into three or more units. The divalent ion-cation vacancy forms a tetragonal defect which can strengthen the lattice through the Fleischer mechanism given in Eq. 1. (5) The $C^{\frac{1}{2}}$ dependence is expected to occur if the moving dislocations can sample the individual defects separately. Such behavior will take place if the defects are isolated or if they are clustered in a suitable orientation such as the long [100] Cl^o needles in irradiated KCl.

We have measured the resolved flow stress, τ_r, for a series of our own Sr doped KCl and Eu doped KCl single crystals. The measurements were made under compression on cleaved [100] samples as described above. The Sr content was determined by atomic absorption spectroscopy and the Eu content was found from the 243nm absorption band as described in the crystal growth section of this report. The results of the measurements are shown in Fig. 3.

The results on KCl:Sr have been reported earlier, (15) as shown in Fig. 4. We find that the increase in τ_r is proportional to the square root of the Sr concentration for our as grown crystals. In contrast, Dryden et al.(14)

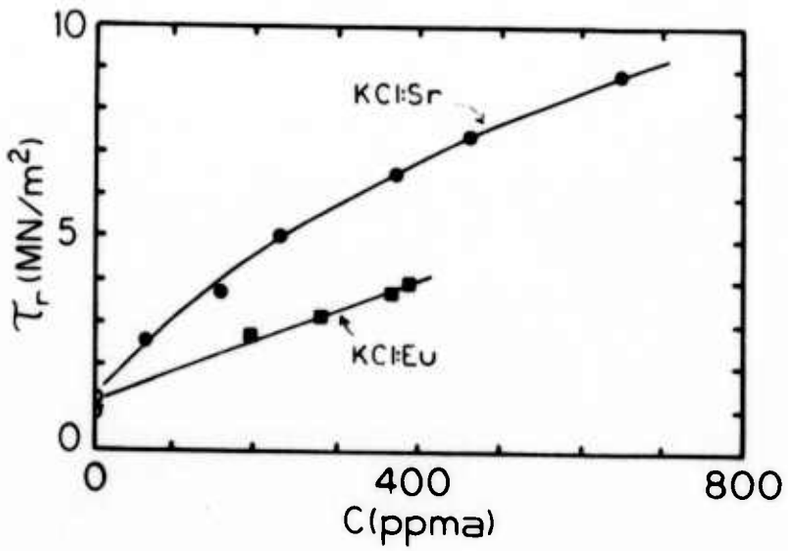

Figure 3. The resolved flow stress of single crystal KCl:Sr and KCl:Eu is shown as a function dopant concentration, C. KCl:Sr has a $C^{\frac{1}{2}}$ dependence while KCl:Eu is linear in C.

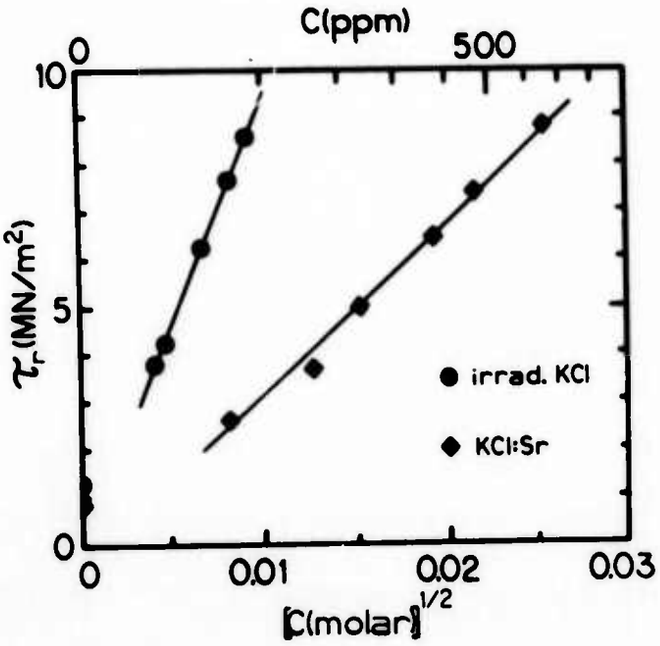

Figure 4. The resolved flow stress of KCl:Sr and irradiated KCl is shown as a function of the square root of the defect concentration.

found a $C^{2/3}$ dependence for KCl:Sr and other doped alkali halides. They also found that the flow stress was sensitive to heat treatment. The results for our KCl:Sr crystals suggest that the moving dislocations are able to sample individual defects which implies that the Sr^{++}-K^{+} vacancy pairs are in a low state of aggregation.

The results for KCl:Eu are also shown in Fig. 3. Eu^{++} in KCl appears to be a less effective strengthening agent than Sr^{++}. In contrast to the $C^{\frac{1}{2}}$ dependence for KCl:Sr we observe a linear relation between the flow stress and the Eu content. Young and Halliburton (16) have made epr measurements on our KCl:Eu crystals. They found that the Eu^{++} ion is paired with the K^{+} vacancy. Our flow stress results indicate that there is some degree of aggregation between the Eu^{++}-K^{+} vacancy pairs.

Figure 4 compares the flow stress of Sr doped KCl and irradiated KCl, both show the $C^{\frac{1}{2}}$ dependence. Doping with divalent ions is seen to be much less effective for strengthening KCl than radiation damage. However, for CO_2 window applications it should be noted that the Sr^{++} doping does not degrade the 10.6μm absorption whereas radiation damage does.

D. Temperature Dependence of the Yield Strength of KCl:Sr and KBr_xCl_{1-x} Crystals.

The temperature dependence of the mechanical strength of candidate window materials is an important parameter. Consequently, we have measured the resolved flow stress, τ_r, of pure and Sr doped KCl and of KBr_xCl_{1-x} crystals from 300 to 700 K.

Mechanical samples similar to those described above were cleaved from pulled ingots. The two KCl-Sr ingots were grown at OSU from RAP KCl and doubly recrystallized $SrCl_2$. The high purity KCl ingot was obtained from the Research Materials Program of the Oak Ridge National Laboratory *sic*, and the KBr_xCl_{1-x}

crystals were obtained from AFCRL. The high-purity crystal was certified by the supplier to have less than 1μg/g total divalent cation concentration. The Ca and Sr content of the Sr doped samples was measured at OSU by atomic absorption spectroscopy.

A number of samples measuring 2 x 2 x 7 mm were cleaved from each ingot. Five samples from each ingot were then randomly selected for testing at each temperature. This minimized systematic errors due to sample dependent sources such as local strains or dopant gradients. Engineering flow stresses were taken to be the value at the intersection of the elastic and first plastic-flow portions of the curve. The results for all five samples were averaged to obtain the values reported for each ingot at each temperature. For the Rocksalt system, $\tau_r = \frac{1}{2} \tau_e$.

The flow stresses were measured under compression on a modified Instron testing machine at a cross-head speed of 0.05 cm/min. The Instron machine was modified by adding a heated anvil and platen. Each consisted of a stainless steel rod 13 cm long by 1.5 cm diameter with a noninductively wound sheathed Nichrome heater on the last 2.5 cm. A polished stainless steel radiation shield attached to the upper anvil heater could be lowered around the work area. Copper-constantan thermocouples were attached to both jaws. The lower (load cell) jaw was electronically controlled to $\pm 1^{o}C$, while the upper anvil was manually controlled to within $\pm 2^{o}C$. After a sample was placed on the platen it was allowed to equilibrate for five minutes.

Figure 5 shows the resolved flow stress of high purity KCl, of KCl + 200 ppm Sr and KCl + 600ppm Sr. The error bars are the rms deviations of the test data. The room temperature flow stresses of the samples are in good agreement with our earlier data. (4) In the as-grown condition - annealed and slow cooled- which is shown by the solid curve the doped samples show a somewhat erratic

behavior for temperatures below 450K, above which, τ_r falls smoothly with increasing temperature. Because of the uncertainty in the data at the higher temperatures, it is not apparent whether the τ_r's for the three samples are converging to a common curve or whether each is asymptotically approaching a value still determined by the dopant concentration. For samples quenched in a few seconds to room temperature after several hours at 650°C, τ_r follows the dashed curves at the lower temperatures and converges to the original curves at the higher temperatures.

The hardening mechanisms for alkali halides doped with divalent impurities are now generally understood. (12,17,18) When divalent cations are added to alkali halides, cation vacancies are formed to maintain charge neutrality. At room temperature most of the vacancies are paired with the divalent impurities (14) the resulting pairs may cluster together. If the moving dislocations interact with isolated divalent cation-cation pairs the $C^{\frac{1}{2}}$ dependence for the flow stress should result. (5) However, clusters of pairs and precipitates may drastically alter this result. (14,17) Because the degree of aggregation will strongly depend upon the samples thermal history and upon the details of the lattice-impurity interaction it is not surprising that widely differing behaviors may be found among the various alkali halides doped with Mg, Ca, Sr or Ba, or between slow cooled and quenched specimens, as found in this study.

While the purpose of this study was to investigate the general behavior of the strength of KCl:Sr crystals as a function of temperature for engineering purposes several observations can be made on the probable nature of the hardening centers.

If we apply Eq. 1 to the 300-450K regime τ_r's with the appropriate shear modules given in Eq. 3 we find an n value of 40 to 50 in the as-grown crystals

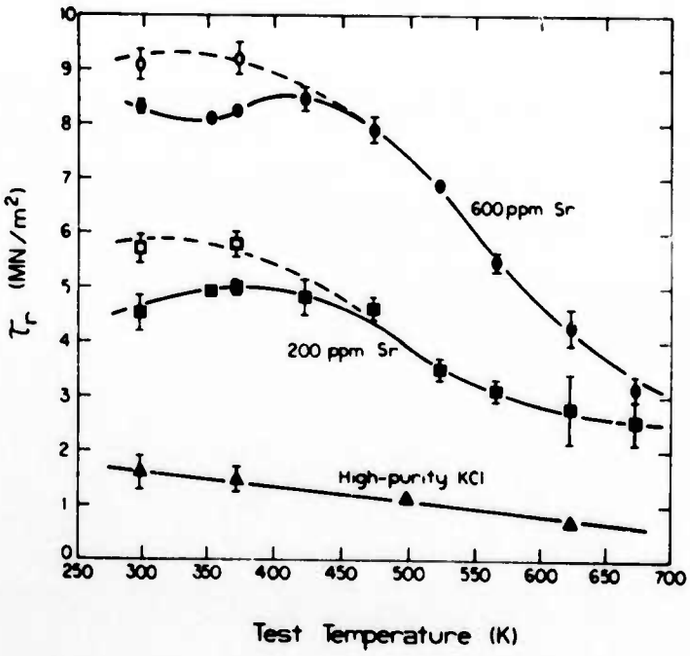

Figure 5. The resolved flow stress for high-purity KCl and two KCl:Sr crystals is shown as a function of temperature.

and about 30 for the quenched samples. For the high temperature data (650-700K) we find an n of 70 to 80. The n value for the low temperature data would be characteristic of small aggregates or other highly assymetric centers while the high temperature result is more characteristic of vacancies or isolated impurities. It should be noted that the divalent impurity-cation vacancy pair would be expected to break up at higher temperatures as would precipitates. Overaging or similar phenomena are probably active in the KCl:Sr system. (17)

The KBr_xCl_{1-x} alloy crystals have a much simpler behavior with temperature as shown in Fig. 6. Slagle and McKinstry (19) found that the shear modules for this system may be approximately represented by

$$G_x(T) = G_{ox}(1 - \alpha\Delta T) \qquad (4)$$

where x is the Br fraction, G_{ox} is the shear modules at 300K, α is the temperature and ΔT is T-300K. coefficient of the shear modules. A similar treatment may be applied to the resolved yield stress.

$$\tau_{rx}(T) = \tau_{rox}[1 - \beta\Delta T] = G_x(T)\,F(T) \qquad (5)$$

where β is the T coefficient of the resolved yield stress for the alloy. Eq. 5 also indicates the relationship to $G_x(T)$ where F(T) contains any other T dependent terms in the strengthening mechanism not included in G_o. Table II compares α and β for the five alloy crystals. The column labeled "% diff" is the percentage difference between α and β using α as the standard quantity.

The change in $G_x(T)$ with temperature does not satisfactorily account for observed change in τ_r for pure KCl. One or more additional softening mechanism must be operative in this crystal which had not been annealed. The alloy crystals which had been annealed prior to use have better agreement between α and β (20 to 40%). Thus the change of τ_r for these crystals is mostly due to $G_x(T)$.

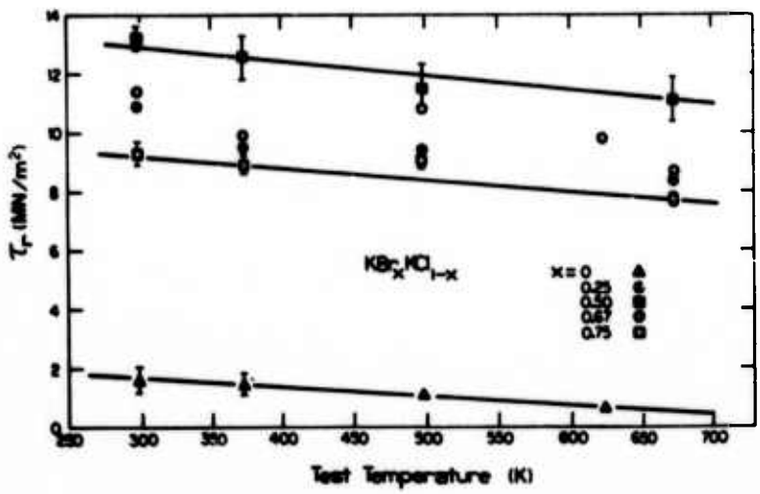

Figure 6. The temperature dependence of the resolved flow stress for KBr_xCl_{1-x} crystals is shown.

TABLE II

Comparison of Temperature Coefficients of the Shear Modules and Resolved Yield Stress for $KB_{rx}KCl_{1-x}$ alloys.

x	α (ppm) (K^{-1})	β (ppm) (K^{-1})	% diff.
0.00	603	1,750	190
0.25	686	561	18
0.50	634	434	32
0.67	695	503	28
0.75	677	404	40

It is interesting to apply Eq. 1 to the data shown in Fig. 2 even though the minority constituent can hardly be called a dopant. Taking C to be the minority concentration gives n = 550 to within $\pm$ 5% for all four alloys and to within $\pm$2% for three. The alloy β with x = 0.5 was considered with both Cl and Br as the minor constituent; thus, effectively giving five alloys. The strengthening mechanism for a solid solution is known to arise from the extra force required to move a dislocation past a "foreign" ion at a lattice site over that necessary to move it past a "host" ion. The large n value indicates that the hardening center is nearly identical to the host ion, simply a different halide. The fact that the x = 0.5 alloy displays the same behavior indicates that the $C^{\frac{1}{2}}$ mechanism holds even when, statistically every other ion is a different type. The $C^{\frac{1}{2}}$ dependence arises if the dislocation line samples each hardening center only once and separately from all others. Thus the same value of n for x = 0.5 as for the other x values implies that the core of a dislocation has a strain field extending only over a distance comparable to or less than the distance between adjacent anions in the $KBr_{0.5}$ $Cl_{0.5}$ lattice.

E. References

1. Air Force Cambridge Research Laboratory Quarterly Progress Report No. 6, AFCRL-72-0559. Special Reports No. 147, September 1972.

2. R. J. Stokes and C. H. Li in Materials Science Research, H. H. Studelmaier and W. W. Austin, ed., (Plenum, N.Y. 1963) Vol. I, pp. 133-157.

3. P. F. Becher and R. W. Rice, J. Appl. Phys. 44, 2915 (1973).

4. W. A. Sibley et al., Annual Technical Report, AFCRL-TR-73-0342, April, 1973.

5. R. L. Fleischer, Acta Met. 10, 835 (1962).

6. J. R. Hopkins, J. A. Miller and J. J. Martin, Phys. Stat. Sol. (a) 19, 591 (1973).

7. W. A. Sibley and J. R. Russell, J. Appl. Phys. 36, 810 (1965).

8. W. A. Sibley and E. Sonder, J. Appl. Phys. 34, 2366 (1963).

9. J. S. Nadeau, J. Appl. Phys. 34, 2248 (1963).

10. J. R. Hopkins, Phys. Stat. Sol. (a) 18, k 15 (1973).

11. L. W. Hobbs, A. E. Hughes and D. Pooley, Proc. Roy. Soc. Lond. A332, 167 (1973).

12. L. W. Hobbs and D. G. Howitt, Paper presented at Europhysical Topical Conference on Lattice Defects in Ionic Crystals, Marseille-Luminey 2-6 July, 1973.

13. P. F. Becher, et al. Third Conference on High Power Infrared Laser Window Materials, C. A. Pitha, A. Armington and H. Posen, eds., Nov. 12-14, 1973. AFCRL-TR-74-0085 (II) Special Reports, No. 174, 14 Feb. 1974.

14. J. S. Dryden, Setsu Morimoto and J. S. Cook, Phil. Mag. 12, 379 (1965).

15. W. A. Sibley et al. Annual Technical Report No. 1, AFCRL-TR-73-0342, 30 April 1973.

16. M. Young and L. E. Halliburton, Oklahoma State University, private communication, 1975.

17. C. Y. Chin, et al. J. Amer. Ceram. Soc. 56, 369 (1973).

18. W. G. Johnston, J. Appl. Phys. 33, 2050 (1962).

19. O. D. Slagle and H. A. McKinstry, J. Appl. Phys. 38, 446 (1967).